The Journal of Chemical Physics

Connecting density fluctuations and Kirkwood–Buff integrals for finite-size systems

Cite as: J. Chem. Phys. **156**, 044502 (2022); https://doi.org/10.1063/5.0076744
Submitted: 27 October 2021 • Accepted: 29 December 2021 • Accepted Manuscript Online: 03 January 2022 • Published Online: 24 January 2022

Mauricio Sevilla and Robinson Cortes-Huerto

The Journal of Chemical Physics ARTICLE scitation.org/journal/jcp

Connecting density fluctuations and Kirkwood–Buff integrals for finite-size systems

Cite as: J. Chem. Phys. 156, 044502 (2022); doi: 10.1063/5.0076744
Submitted: 27 October 2021 • Accepted: 29 December 2021 •
Published Online: 24 January 2022

Mauricio Sevilla and Robinson Cortes-Huerto[a)]

AFFILIATIONS

Max Planck Institute for Polymer Research, Ackermannweg 10, 55128 Mainz, Germany

[a)]Author to whom correspondence should be addressed: corteshu@mpip-mainz.mpg.de

ABSTRACT

Kirkwood–Buff integrals (KBIs) connect the microscopic structure and thermodynamic properties of liquid solutions. KBIs are defined in the grand canonical ensemble and evaluated by assuming the thermodynamic limit (TL). In order to reconcile analytical and numerical approaches, finite-size KBIs have been proposed in the literature, resulting in two strategies to obtain their TL values from computer simulations. (i) The spatial block analysis method in which the simulation box is divided into subdomains of volume V to compute density fluctuations. (ii) A direct integration method where a corrected radial distribution function and a kernel that accounts for the geometry of the integration subvolumes are combined to obtain KBI as a function of V. In this work, we propose a method that connects both strategies into a single framework. We start from the definition of finite-size KBI, including the integration subdomain and an asymptotic correction to the radial distribution function, and solve them in Fourier space where periodic boundary conditions are trivially introduced. The limit $q \to 0$, equivalent to the value of the KBI in the TL, is obtained via the spatial block-analysis method. When compared to the latter, our approach gives nearly identical results for all values of V. Moreover, all finite-size effect contributions (ensemble, finite-integration domains, and periodic boundary conditions) are easily identifiable in the calculation. This feature allows us to analyze finite-size effects independently and extrapolates the results of a single simulation to different box sizes. To validate our approach, we investigate prototypical systems, including SPC/E water and aqueous urea mixtures.

I. INTRODUCTION

Kirkwood–Buff integrals (KBIs) connect the microscopic structure of a liquid solution, via integrals of the radial distribution functions (RDFs), and its thermodynamic properties, as obtained from fluctuations of the number of particles in subvolumes of the total system.[1] This connection between local structure and thermodynamics is particularly useful in computational soft-matter studies where KBIs are widely used to evaluate isothermal compressibility, partial molar volumes, and derivatives of chemical potentials.[2–5] In particular, applications of KBI include the investigation of the thermodynamics of complex molecular mixtures,[6–12] solvation of macromolecules,[13–20] multicomponent diffusion in liquids,[21,22] protein self-assembly and aggregation,[23,24] Hofmeister ion chemistry,[25] identification of nanostructures in water solutions of ionic liquids,[26] and the parameterization of atomistic[27–30] and coarse-grained[31,32] force fields. Recently, KBIs have been applied to compute isothermal compressibility of prototypical crystals,[33,34] showing unprecedented flexibility and range of applicability.

KBIs are strictly defined in the grand canonical ensemble. Moreover, in practice, it is usual to take the thermodynamic limit (TL) to reduce their calculation to spherically symmetric real-space integrals of the radial distribution functions. In computer simulations, the TL is approximated by introducing periodic boundary conditions (PBC) for a system with a fixed number of particles N_0. Accordingly, finite subvolumes V with an average number of particles $\langle N \rangle$ are used to compute fluctuations of the number of particles and radial distribution functions.[35,36] Periodicity, different thermodynamic ensembles and finite integration domains introduce artifacts in the resulting KBI.

Finite-size KBIs have been proposed in the literature to bridge the existing gap between analytical expressions and numerical

studies. Similar to the definition in the grand canonical ensemble, finite-size KBIs equate fluctuations of the number of particles in subvolumes V inside the simulation box with integrals of the corresponding closed-system radial distribution functions.[37–39] This relation provides two routes to obtain KBI in the TL. The first one, i.e., the spatial block analysis method (SBA), is based on calculating fluctuations of the number of particles in subdomains of volume V. By using arguments from the thermodynamics of small systems,[35] linear scaling relations are defined to extrapolate KBI in the TL.[40,41] The second possibility is to correct the radial distribution functions for the differences in the thermodynamic ensemble and then integrate them using a kernel that takes into account finite-size domains.[42–45] Naturally, the limit $V \to \infty$ gives the KBI in the TL.

Indeed, the two approaches are connected. In the limit $V > V_\zeta$, with the volume V_ζ defined by the correlation length of the system ζ, the integration of the radial distribution functions gives an expression equivalent to the result obtained from linear scaling of fluctuations of the number of particles, including ensemble and finite integration domain effects.[46] Nevertheless, the local solvation structure information, provided by the short-range part of the RDF, is lost in this case. Moreover, the effect of periodic boundary conditions is not included in the final result.

In this work, we propose a method that connects the spatial block analysis method to the direct integration of exact finite-size KBI. We evaluate the large r limit by introducing an asymptotic correction to the RDF. By defining the geometry of the subdomain, we write and solve KBI in Fourier space where the periodicity of the cell can also be incorporated, following the procedure proposed in Ref. 47. We compute the $q \to 0$ limit by using the spatial block analysis method. We thus obtain KBI as a function of the volume of the subdomain and find excellent agreement with fluctuations of the number of particles for SPC/E water and aqueous urea mixtures for all values of V. The method is accurate, and its implementation is straightforward. It simply requires performing a spatial block analysis and calculating one-dimensional integrals of partial structure factors.

This paper is organized as follows: In Sec. II, we introduce the method, and in Sec. III, we give the computational details. We present the main results in Sec. IV and conclude in Sec. V.

II. KIRKWOOD–BUFF INTEGRALS FOR FINITE-SIZE SYSTEMS

For a multicomponent fluid of species i, j, contained in a volume $V = L^3$, in thermal and chemical equilibrium with an infinite reservoir of particles, the Kirkwood–Buff integral (KBI) is defined as[1]

$$G_{ij} = V\left(\frac{\langle N_i N_j\rangle - \langle N_i\rangle\langle N_j\rangle}{\langle N_i\rangle\langle N_j\rangle} - \frac{\delta_{ij}}{\langle N_i\rangle}\right) = \frac{1}{V}\int_V\int_V d\mathbf{r}_1 d\mathbf{r}_2 [g_{ij}(\mathbf{r}) - 1], \quad (1)$$

where N_i is the number of particles of the i species, the bracket $\langle\cdots\rangle$ denotes a thermal average, δ_{ij} is the Kronecker delta, and g_{ij} is the pair correlation function defined in the grand canonical ensemble with $\mathbf{r} = \mathbf{r}_2 - \mathbf{r}_1$.

In computer simulations, we usually investigate systems with fixed number of particles N_0 with volume $V_0 = L_0^3$. Building on similar results for the Ornstein–Zernike equation,[47] we define the finite-size KBI as

$$G_{ij}(V; V_0) = V\left(\frac{\langle N_i N_j\rangle' - \langle N_i\rangle'\langle N_j\rangle'}{\langle N_i\rangle'\langle N_j\rangle'} - \frac{\delta_{ij}}{\langle N_i\rangle'}\right) = \frac{1}{V}\int\int d\mathbf{r}_1 d\mathbf{r}_2\, R(\mathbf{r}_1)\, R(\mathbf{r}_2)\,[g_{ij}(\mathbf{r}; V_0) - 1], \quad (2)$$

where the average $\langle\cdots\rangle' \equiv \langle\cdots\rangle_{V,V_0}$ now explicitly depends on the subdomain and total volumes, V and V_0, respectively (see Fig. 1). Here, we focus on the integral term that contains the radial distribution function of the closed system, $g_{ij}(\mathbf{r};\ V_0)$, and a step function $R(\mathbf{r})$ that defines the integration subdomain: it is one inside and zero outside the volume V. By defining Eq. (2), we connect explicitly density fluctuations and the integral of the pair correlation function for any subdomain V.

In the following, we focus on integrating the rhs of Eq. (2), that is,

$$G_{ij}(V; V_0) = \frac{1}{V}\int\int d\mathbf{r}_1 d\mathbf{r}_2\, R(\mathbf{r}_1)\, R(\mathbf{r}_2)\, h_{ij}(\mathbf{r}; V_0), \quad (3)$$

with $h_{ij}(\mathbf{r};\ V_0) = g_{ij}(\mathbf{r};\ V_0) - 1$.

To include the correction due to ensemble effects, we use the approximation proposed in Ref. 46,

$$g_{ij}(\mathbf{r}; V_0) = g_{ij}(\mathbf{r}) - \frac{1}{V_0}\left(\frac{\delta_{ij}}{\rho_i} + G_{ij}^{\infty}\right), \quad (4)$$

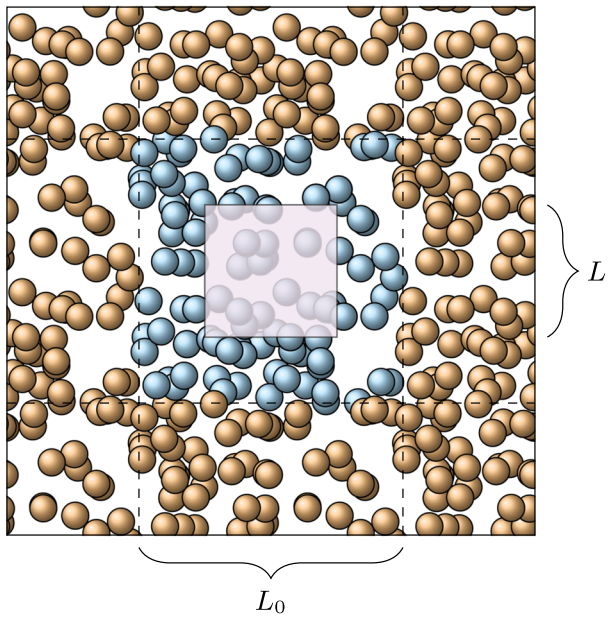

FIG. 1. Schematic representation of the spatial block analysis method. The N_0 blue particles represent the system with linear size L_0, and the red particles represent the periodic images. The purple box is a subvolume of linear size $L < L_0$ defined to compute fluctuations of the number of particles.

based on the asymptotic limit $g_{ij}(r \to \infty; V_0) = 1 - (\delta_{ij}/\rho_i + G_{ij}^{\infty})/V_0$ discussed in Ref. 2. This implies that

$$h_{ij}(\mathbf{r}; V_0) = h_{ij}(\mathbf{r}) - \frac{1}{V_0}\left(\frac{\delta_{ij}}{\rho_i} + G_{ij}^{\infty}\right), \tag{5}$$

and, thus, the finite-size KBI becomes

$$G_{ij}(V; V_0) = G_{ij}(V) - \frac{V}{V_0}\left(\frac{\delta_{ij}}{\rho_i} + G_{ij}^{\infty}\right), \tag{6}$$

where the second term on the rhs contains the correction due to ensemble effects[3,4,46,48] and

$$G_{ij}(V) = \frac{1}{V}\int\int d\mathbf{r}_1 d\mathbf{r}_2\, R(\mathbf{r}_1)\, R(\mathbf{r}_2)\, h_{ij}(\mathbf{r}). \tag{7}$$

This expression can be easily written in Fourier space,

$$G_{ij}(V) = \frac{1}{(2\pi)^3 V}\int d\mathbf{k}\, \tilde{R}(\mathbf{k})\, \tilde{R}(-\mathbf{k})\, \tilde{h}_{ij}(\mathbf{k}), \tag{8}$$

where $\tilde{h}_{ij}$ is the Fourier transform of h_{ij}. An additional advantage of integrating in reciprocal space is that periodic boundary conditions can be considered explicitly.[47,49] It is enough to rewrite $\tilde{h}_{ij}(\mathbf{k})$ such that periodic copies of the system are included via a phase factor. That is, we include the complete contribution of the periodic boundary conditions into Eq. (8) as

$$G_{ij}(V) = \frac{1}{(2\pi)^3 V}\int d\mathbf{k}\, \tilde{R}(\mathbf{k})\, \tilde{R}(-\mathbf{k})\, \tilde{h}_{ij}^{\mathrm{PBC}}(\mathbf{k}), \tag{9}$$

where[47]

$$\tilde{h}_{ij}^{\mathrm{PBC}}(\mathbf{k}) = \sum_{n_x,n_y,n_z} e^{-\mathbf{k}\cdot\mathbf{s}_{n_x,n_y,n_z}}\, \tilde{h}_{ij}(\mathbf{k}), \tag{10}$$

with $\mathbf{s}_{n_x,n_y,n_z} = (n_x L_{0x}, n_y L_{0y}, n_z L_{0x})$, a vector specifying the system's periodic images such that $n_{x,y,z}$ takes integer values. In the following, we consider a cubic simulation box with $L_{0x} = L_{0y} = L_{0z} = L_0$. Moreover, we find that the choices $|n_x| \le 1$, $|n_y| \le 1$, and $|n_z| \le 1$ are sufficient to compute Eq. (9) accurately.

We assume a homogeneous and isotropic fluid such that $\tilde{h}_{ij}(\mathbf{k}) = \tilde{h}_{ij}(k)$ with $k = \sqrt{\mathbf{k}\cdot\mathbf{k}}$. Hence, in practice, we use the relation between $\tilde{h}_{ij}(k)$ and the partial structure factors S_{ij},[50,51] namely,

$$S_{ij}(k) = \delta_{ij} + \tilde{h}_{ij}(k). \tag{11}$$

The partial structure factors are computed as[26,52,53]

$$S_{ij}(\mathbf{k}) = \frac{1}{N}\left\langle \sum_{i'\in i}^{N_i}\sum_{j'\in j}^{N_j} \exp(-i\mathbf{k}\cdot(\mathbf{r}_{i'} - \mathbf{r}_{j'}))\right\rangle. \tag{12}$$

The average in the previous equation runs over values of $\mathbf{k}$ such that $|\mathbf{k}| = k$ as well as over the simulation ensemble. Consequently, the problem reduces to evaluate a single integral of the partial structure factors given by Eq. (9).

In principle, Eq. (6) now includes all the finite-size effects present in the simulation (finite boundary, periodicity of the box, and ensemble). Before entering into applications, there are still two issues demanding our immediate attention. The first is that the asymptotic correction in Eq. (6) requires the value of G_{ij}^{∞}. The second concerns the evaluation of $\lim_{k\to 0} S_{ij}(k)$ that reduces, again, to evaluate G_{ij}^{∞}. Indeed, we have

$$\lim_{k\to 0} S_{ij}(k) = \delta_{ij} + \rho_i\, G_{ij}^{\infty}. \tag{13}$$

To obtain G_{ij}^{∞}, we recall that, in the limit $V_\zeta < V < V_0$ (grand canonical ensemble), Eq. (7) can be approximated to $G_{ij}(V) \approx G_{ij}^{\infty} + \alpha_{ij}/V^{1/3}$,[37,38,40,42] where α_{ij} is a constant. By including this approximation into Eq. (6), we recover the spatial block analysis (SBA) result consistent with the result reported in Ref. 46,

$$G_{ij}^{\mathrm{SBA}}(V; V_0) = G_{ij}^{\infty}\left(1 - \frac{V}{V_0}\right) - \frac{V}{V_0}\frac{\delta_{ij}}{\rho_i} + \frac{\alpha_{ij}}{V^{1/3}}. \tag{14}$$

By evaluating density fluctuations for volumes $V \le V_0$, as defined by the left-hand side of Eq. (2), it is thus possible to extrapolate G_{ij}^{∞}.[40,46]

To summarize, the present method to evaluate KBI for finite systems requires information readily accessible from the simulation trajectory: density fluctuations for subvolumes $V \le V_0$ and partial structure factors. Additional corrections to the RDF or finite domain integration kernels are not required. Moreover, periodic boundary effects are trivially included in the calculation.

III. COMPUTATIONAL DETAILS

To validate our approach, we first focus on liquid SPC/E water.[54] Molecular dynamics simulations have been carried out with GROMACS 4.5.1[55] for systems containing 1000 and 8000 water molecules. We started with systems of initial density ≈26 waters/nm^3 (≈776 kg/m^3) that were optimized using steepest descent minimization (50 000 steps are sufficient). An equilibration run of 3.5 ns was carried out in the NPT ensemble at 1 bar. Next, we alternated 3.5 ns (time step = 1 fs) constant pressure (NPT) at P = 1 bar and constant volume (NVT) simulations at T = 300 K. For NPT simulations, we used the Berendsen barostat,[56] and for NVT simulations, the temperature was enforced by a velocity rescaling thermostat.[57] We continued with this protocol until we verified that in the NPT ensemble, the density is 33.5 waters/nm^3 (1000 kg/m^3) and that in the NVT simulation, pressure fluctuates around the 1 bar value. The last NVT trajectory obtained after this sequence of NPT–NVT equilibration runs was used for the spatial block analysis and for the calculation of the structure factor.

To test the method with a multicomponent case, we have reused our simulation trajectories of aqueous urea solution[4,32] using the Kirkwood–Buff derived force field[58] and SPC/E water[54] in GROMACS 4.5.1[55] with a relatively small size of the simulation box ($L \sim 8$ nm). We have considered four more molar concentrations for a total of seven molar concentrations: 2.00, 3.06, 3.90, 5.07, 6.03, 7.10, and 8.03M. Hence, we have alternated 3.5 ns (time step = 1 fs) constant pressure (NPT) at P = 1 bar and constant volume (NVT) simulations at T = 300 K. For NPT simulations, we used a Berendsen barostat[56] to control the pressure, and for NVT simulations, a velocity rescaling thermostat[57] to enforce the target temperature. We continued with this protocol (38 NPT–NVT cycles) until we verified that in the NVT simulation, pressure fluctuates around 1 bar. Also in this case, the last NVT trajectory obtained after this NPT–NVT equilibration sequence was used for the spatial block analysis and for the calculation of the partial structure factors.

IV. RESULTS

A. Single-component liquid: SPC/E water

For the single-component liquid, we focus on the Ornstein–Zernicke integral equation for finite-size systems.[37,59–61] For a closed system with fixed number of particles N_0 and volume V_0, including PBC. Similar to Eq. (2), we define[47,48]

$$\chi_T(V;V_0) = \frac{\langle N^2\rangle' - \langle N\rangle'^2}{\langle N\rangle'} = 1 + \frac{\rho}{V}\int_V\int_V d\mathbf{r}_1 d\mathbf{r}_2 R(\mathbf{r}_1)R(\mathbf{r}_2)[g(\mathbf{r};V_0)-1], \quad (15)$$

and in this case, we use the asymptotic correction to the RDF proposed in Refs. 60 and 62,

$$g(\mathbf{r};V_0) = g(\mathbf{r}) - \frac{\chi_T^\infty}{N_0}, \quad (16)$$

by neglecting $O(1/N_0^2)$ contributions. $\chi_T^\infty = \rho k_B T \kappa_T$, where κ_T being the isothermal compressibility of the bulk system. To solve the integral on the rhs of Eq. (15), we use the same procedure as described in Sec. II. In cases where $V_\zeta < V < V_0$, we obtain the equivalent spatial block analysis expression,[3,4]

$$\chi_T^{\mathrm{SBA}}(V;V_0) = \chi_T^\infty\left(1-\frac{V}{V_0}\right) + \frac{\rho\alpha}{V^{1/3}}, \quad (17)$$

with α a constant.

First, we compute density fluctuations as defined on the l.h.s. of Eq. (15) for both $N_0 = 1000$ and 8000 systems. By defining $\lambda = (V/V_0)^{1/3}$, we plot $\lambda\chi_T$ as a function of λ (Fig. 2). We extrapolate χ_T^∞ from the curve's slope in the region $\lambda < 0.3$ for the system with $N_0 = 8000$ water molecules. The choice of this linear region is motivated by the fact that $\lambda\chi_T$, as obtained from Eq. (15), has the maximum at $\lambda_{\max} = 0.63$. Thus, we estimated $\lambda = 0.3$ as the value where the curve starts deviating significantly from a straight line. We can also use $\lambda = 0.3$ to choose an appropriate size of the system for the spatial block analysis. By assuming that the correlation length of water is $\zeta = 1.5$ nm, we define $V_\zeta^{1/3} = 1.5\times(4\pi/3)^{1/3}$ nm. The simulation box with $N = 8000$ water molecules has $V_0^{1/3} = 6.2$ nm, thus $\lambda = (V_\zeta/V_0)^{1/3} = 0.39$. This value is larger than $\lambda = 0.3$; still, it is sufficient to obtain a value of $\chi_T^\infty = 0.062$, in good agreement with the results reported in Ref. 4. In practice, to select the size of the system, one can start by estimating the correlation length from the radial distribution function and evaluating the linear size of the box such that $\lambda \approx 0.3$. This criterion can also be applied to binary mixtures.

We use the results of this linear fit to plot the SBA results [Eq. (17)]. Also for this system, we compute the structure factor and correct for the $\lim_{k\to 0}$ by using the relation,

$$\lim_{k\to 0} S(k) = \chi_T^\infty. \quad (18)$$

We, thus, compute an integral equivalent to Eq. (8) to obtain $\chi_T(V;V_0)$. The results for both systems are also presented in Fig. 2. It is apparent that the agreement between density fluctuations and the integral method presented here is excellent. In contrast to the spatial block analysis result [Eq. (17)], oscillations of $\lambda\chi_T$ at low values of λ, related to the local liquid structure, and at large values of λ, due to the periodicity of the simulation box, are consistently reproduced with our method. This is particularly interesting for the system with $N_0 = 1000$ water molecules, where oscillations are more pronounced. In this case, our integral method uses information from the system with $N_0 = 8000$ water molecules. The small box behavior is reproduced *artificially* via the periodic images in Eq. (10).

We now focus on the different finite-size effects present in the system with $N_0 = 1000$ water molecules. In Fig. 3, we present four possibilities of evaluating the rhs of Eq. (15). (i) For the closed system, i.e., including the correction $\chi_T^\infty V/V_0$, with PBC, we observe that $\chi_T(\lambda = 1) = 0$, as expected. (ii) The closed system without PBC gives a limit $\chi_T(\lambda = 1) = \rho\alpha/V_0^{1/3}$ consistent with Eq. (17). (iii) An open system can be obtained by neglecting the correction $\chi_T^\infty V/V_0$. Moreover, by including PBC, we obtain $\chi_T(\lambda = 1) = \chi_T^\infty = 0.062$,

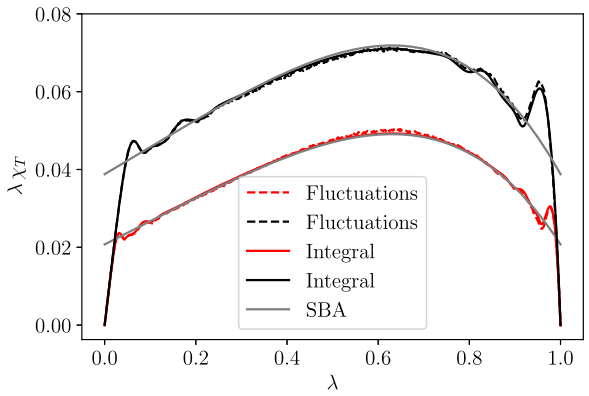

FIG. 2. Plots of the normalized finite-size isothermal compressibility $\lambda\chi_T$ as a function of $\lambda = (V/V_0)^{1/3}$ for systems with $N_0 = 1000$ (black) and 8000 (red) water molecules. Dashed lines correspond to density fluctuations and solid lines represent the method presented here. Solid gray lines correspond to the fitting of Eq. (17).

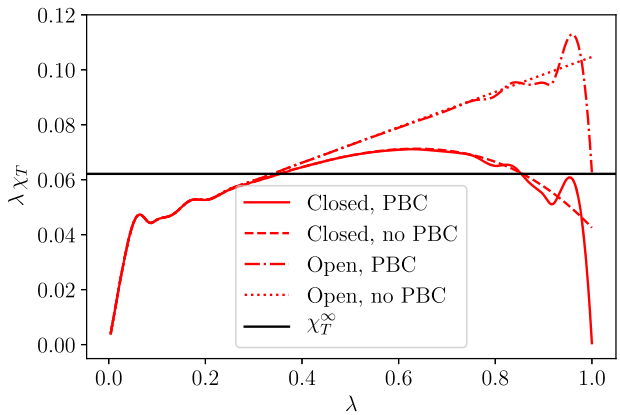

FIG. 3. Calculation of $\lambda\chi_T$ with our method [Eq. (9)] for the system with $N_0 = 1000$ molecules. We present four cases: (solid) closed system with PBC, (dashed) closed system without PBC, (dashed-dotted) open system with PBC, and (dotted) open system without PBC. The black horizontal line corresponds to $\chi_T^\infty = 0.062$.

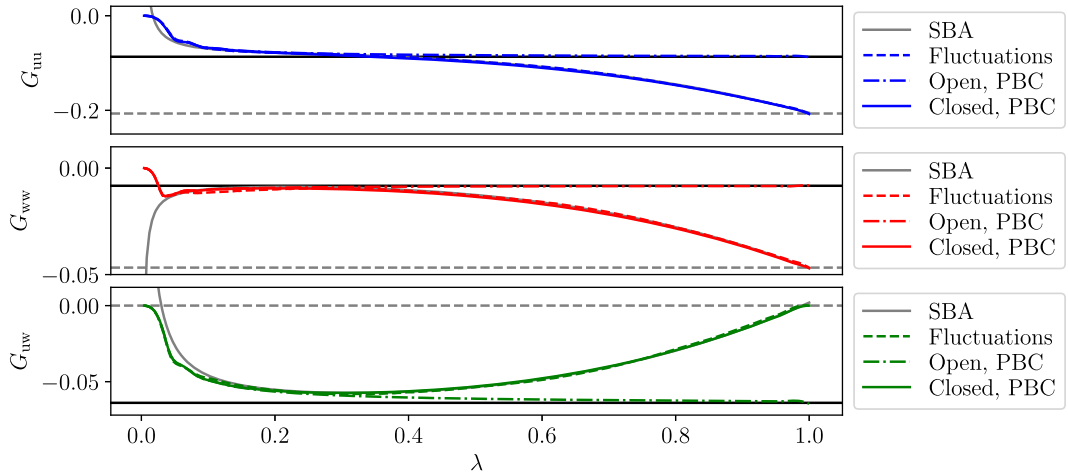

FIG. 4. KBI components G_{uu} (blue, top panel), G_{ww} (red, middle panel), and G_{uw} (green, bottom panel) for an 8M aqueous urea mixture as a function of $\lambda = (V/V_0)^{1/3}$. We present density fluctuations as obtained from the left-hand side of Eq. (2) (dashed lines), the spatial block analysis approximation in Eq. (14) (gray lines), and from the finite KBI expression [Eq. (6)] with $G_{ij}(V)$ given by the Fourier integral [Eq. (9)] with (solid) and without (dashed-dotted lines) the correction to ensemble effects given by $G_{ij}^{\infty}\lambda^3$. The solid black lines correspond to the KBI in the TL, G_{ij}^{∞}. The dashed gray lines indicate the asymptotic limit for the closed system, $-\delta_{ij}/\rho_i$.

precisely the thermodynamic limit value. (iv) For an open system without PBC, $\chi_T(\lambda = 1) = \chi_T^{\infty} + \rho\alpha/V_0^{1/3}$, again consistent with Eq. (17). These results thus highlight the role of PBC in enforcing the correct behavior at the boundary of open and closed molecular systems.

B. Binary mixture: Aqueous urea solution

We perform a similar analysis for the aqueous urea mixture case. First, we compute fluctuations of the number of particles as defined on the l.h.s. of Eq. (2). As for the single-component case, we define $\lambda = (V/V_0)^{1/3}$ and plot λG_{ij} as a function of λ. We carried out this study for all concentrations. However, we only present the results for the case 8M in Fig. 4 (dashed lines). Using the information from the linear region $\lambda < 0.3$, we extrapolate G_{ij}^{∞} and obtain α_{ij}. In this case, we get $G_{uu}^{\infty} = -0.0867$, $G_{uw}^{\infty} = -0.0639$, and $G_{ww}^{\infty} = -0.0083$ nm^3 with uu, uw, and ww corresponding to urea–urea, urea-water, and water–water components, respectively. These values well reproduce derivatives of activity coefficients reported experimentally,[4,46] as expected from the force field parameterization,[58] as well as excess chemical potentials trends with concentration obtained with different computational methods.[63,64] We insert these values in Eq. (14), i.e., SBA, and plot this result as well (solid gray lines). Finally, we use the finite KBI introduced here [Eq. (6)] and use the Fourier integral [Eq. (9)] to compute $G_{ij}(V)$. We present both results with (solid lines) and without (dashed-dotted lines) the correction to the ensemble finite-size effects, $G_{ij}^{\infty}\lambda^3$.

In this case as well, the results of our method accurately reproduce density fluctuations in the whole range $0 < \lambda < 1$, including both local structure ($\lambda \ll 1$) and periodic boundary ($\lambda \approx 1$) features. As anticipated, it is also apparent that the SBA result does not reproduce these limiting cases. Nevertheless, in the limit $\lambda = 1$, the results from fluctuations, SBA, and our integration (closed, PBC) converge to $-\delta_{ij}/\rho_i$, the expected result of the KBI for a closed system.[2] As previously stated, we can separate finite-size contributions by focusing on the corresponding terms in Eqs. (6) and (9). In particular, for an open system (open, PBC), i.e., $\lim_{V_0\to\infty}$, we verify that the KBIs converge to G_{ij}^{∞} when $\lambda = 1$.

We examine this in more detail in Fig. 5 where the normalized KBI for urea–urea, λG_{uu}, is presented. In addition to the limiting

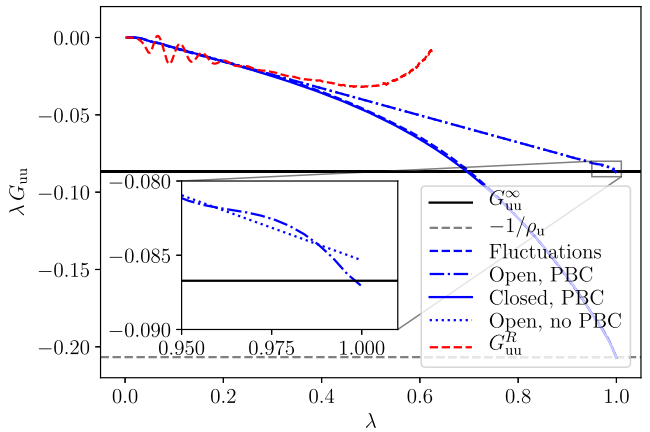

FIG. 5. Normalized KBI, λG_{uu}, as a function of λ obtained using various methods and conditions. Fluctuations—Fluctuations of the number of particles as obtained from the l.h.s. of Eq. (2) (dashed lines). Closed, PBC and Open, PBC—finite KBI expression [Eq. (6)] with $G_{uu}(V)$ given by the Fourier integral [Eq. (9)] with (solid) and without (dashed-dotted lines) the correction to ensemble effects given by $G_{uu}^{\infty}\lambda^3$, both with PBC. Open, no PBC—finite KBI without the correction for the thermodynamic ensemble and without PBC. The solid black line corresponds to the KBI in the TL, G_{uu}^{∞}. The dashed gray line indicates the asymptotic limit for the closed system, $-1/\rho_u$. The red-dashed line corresponds to the running integral [Eq. (19)]. (Inset) Detail of the convergence to the TL.

cases discussed above, we also consider an open system without periodic boundary conditions (dotted line). It is apparent in the region $\lambda \approx 1$ (inner panel) that G_{uu} for an open system with PBC converges to the value in the thermodynamic limit G_{uu}^{∞}, whereas for the open system without PBC, G_{uu} is slightly larger than G_{uu}^{∞} value by a factor $\alpha_{uu}/V_0^{1/3}$, as expected from the SBA expression [Eq. (14)]. As in the single-component case, this result emphasizes that PBC enforces the correct behavior at the boundary of closed and open liquid mixtures. Finally, we also present the normalized running integral λG_{ij}^{R} (red-dashed line) using

$$G_{ij}^{R} = 4\pi \int_0^R dr\, r^2 (g(r; V_0) - 1), \tag{19}$$

with $R > \zeta$, an expression frequently used in the literature. The major differences with the results presented in this work resulting from various finite-size effects highlight the apparent limitations of using such an expression to calculate KBI.

V. CONCLUDING REMARKS

Finite Kirkwood–Buff integrals (KBIs) enable us to sample the thermodynamic limit of liquid mixtures via relatively small computer simulations. The definition of finite KBI balance fluctuations of the number of particles in subdomains within the simulation box and integrals of the corresponding RDF. In this work, we underline this equality by reproducing density fluctuations as a function of the linear size of the subdomain via a simple integration strategy. In particular, we introduce a method to evaluate KBI via integrals of the partial structure factors in reciprocal space combined with the SBA method. A significant advantage of our approach corresponds to the direct inclusion of finite integration domains and PBC contributions. Consequently, we can now identify and *remove* finite-size effects such that grand canonical and thermodynamic limit results become readily available from finite-size computer simulations. Moreover, we show that this scheme enables us to extrapolate our results to different sizes of the simulation box simply by modifying the periodicity factor in the integration procedure. The simplicity of the method is apparent since it only requires fluctuations of the number of particles calculated for different subdomain sizes and the partial structure factors. We foresee immediate applications in situations where PBC plays a pivotal role, namely, the recently introduced KBI for crystalline materials.[33,34]

ACKNOWLEDGMENTS

We are grateful to Kurt Kremer, Debashish Mukherji, and Pietro Ballone for insightful discussions. We also thank Atreyee Banerjee for her critical reading of the manuscript. R.C.-H. gratefully acknowledges funding from SFB-TRR146 of the German Research Foundation (DFG). Simulations have been performed on the THINC cluster at the Max Planck Institute for Polymer Research and on the COBRA cluster of the Max Planck Computing and Data Facility.

AUTHOR DECLARATIONS

Conflict of Interest

There are no conflicts of interest to declare.

DATA AVAILABILITY

The data that support the findings of this study are available from the corresponding author upon reasonable request.

REFERENCES

[1] J. G. Kirkwood and F. P. Buff, "The statistical mechanical theory of solutions. I," J. Chem. Phys. **19**(6), 774–777 (1951).
[2] A. Ben-Naim, *Molecular Theory of Solutions* (Oxford University Press, 2006).
[3] M. Heidari, K. Kremer, R. Potestio, and R. Cortes-Huerto, "Fluctuations, finite-size effects and the thermodynamic limit in computer simulations: Revisiting the spatial block analysis method," Entropy **20**(4), 222 (2018).
[4] M. Heidari, K. Kremer, R. Potestio, and R. Cortes-Huerto, "Finite-size integral equations in the theory of liquids and the thermodynamic limit in computer simulations," Mol. Phys. **116**(21–22), 3301–3310 (2018).
[5] V. Bråten, Ø. Wilhelmsen, and S. K. Schnell, "Chemical potential differences in the macroscopic limit from fluctuations in small systems," J. Chem. Inf. Model. **61**(2), 840–855 (2021).
[6] D. Mukherji, N. F. A. van der Vegt, K. Kremer, and L. Delle Site, "Kirkwood–Buff analysis of liquid mixtures in an open boundary simulation," J. Chem. Theory Comput. **8**(2), 375–379 (2012).
[7] D. Mukherji, N. F. A. van der Vegt, and K. Kremer, "Preferential solvation of triglycine in aqueous urea: An open boundary simulation approach," J. Chem. Theory Comput. **8**(10), 3536–3541 (2012).
[8] A. A. Galata, S. D. Anogiannakis, and D. N. Theodorou, "Thermodynamic analysis of Lennard-Jones binary mixtures using Kirkwood-Buff theory," Fluid Phase Equilib. **470**, 25–37 (2018).
[9] A. Narayanan Krishnamoorthy, C. Holm, and J. Smiatek, "Influence of cosolutes on chemical equilibrium: A Kirkwood–Buff theory for ion pair association–dissociation processes in ternary electrolyte solutions," J. Phys. Chem. C **122**(19), 10293–10302 (2018).
[10] P. C. Petris, S. D. Anogiannakis, P.-N. Tzounis, and D. N. Theodorou, "Thermodynamic analysis of *n*-hexane–ethanol binary mixtures using the Kirkwood–Buff theory," J. Phys. Chem. B **123**(1), 247–257 (2019).
[11] B. Lovrinčević, A. Bella, I. Le Tenoux-Rachidi, M. Požar, F. Sokolić, and A. Perera, "Methanol-ethanol 'ideal' mixtures as a test ground for the computation of Kirkwood-Buff integrals," J. Mol. Liq. **293**, 111447 (2019).
[12] A. T. Celebi, N. Dawass, O. A. Moultos, and T. J. H. Vlugt, "How sensitive are physical properties of choline chloride–urea mixtures to composition changes: Molecular dynamics simulations and Kirkwood–Buff theory," J. Chem. Phys. **154**(18), 184502 (2021).
[13] M. Kang and P. E. Smith, "Preferential interaction parameters in biological systems by Kirkwood–Buff theory and computer simulation," Fluid Phase Equilib. **256**(1), 14–19 (2007).
[14] V. Pierce, M. Kang, M. Aburi, S. Weerasinghe, and P. E. Smith, "Recent applications of Kirkwood–Buff theory to biological systems," Cell Biochem. Biophys. **50**(1), 1–22 (2008).
[15] S. Shimizu, R. Stenner, and N. Matubayasi, "Gastrophysics: Statistical thermodynamics of biomolecular denaturation and gelation from the Kirkwood-Buff theory towards the understanding of tofu," Food Hydrocolloids **62**, 128–139 (2017).
[16] D. Mukherji and K. Kremer, "Coil–globule–coil transition of PNIPAm in aqueous methanol: Coupling all-atom simulations to semi-grand canonical coarse-grained reservoir," Macromolecules **46**(22), 9158–9163 (2013).
[17] E. A. Oprzeska-Zingrebe and J. Smiatek, "Aqueous ionic liquids in comparison with standard co-solutes," Biophys. Rev. **10**(3), 809–824 (2018).
[18] E. A. Oprzeska-Zingrebe, M. Kohagen, J. Kästner, and J. Smiatek, "Unfolding of DNA by co-solutes: Insights from Kirkwood–Buff integrals and transfer free energies," Eur. Phys. J.: Spec. Top. **227**(14), 1665–1679 (2019).

[19]M. Tripathy, S. Bharadwaj, B. Shadrack Jabes, and N. F. A. van der Vegt, "Characterizing polymer hydration shell compressibilities with the small-system method," Nanomaterials **10**(8), 1460 (2020).
[20]E. A. Oprzeska-Zingrebe and J. Smiatek, "Interactions of a DNA G-quadruplex with TMAO and urea: A molecular dynamics study on co-solute compensation mechanisms," Phys. Chem. Chem. Phys. **23**, 1254–1264 (2021).
[21]S. Kjelstrup, S. K. Schnell, T. J. H. Vlugt, J.-M. Simon, A. Bardow, D. Bedeaux, and T. Trinh, "Bridging scales with thermodynamics: From nano to macro," Adv. Nat. Sci.: Nanosci. Nanotechnol. **5**(2), 023002 (2014).
[22]X. Liu, S. K. Schnell, J.-M. Simon, P. Krüger, D. Bedeaux, S. Kjelstrup, A. Bardow, and T. J. H. Vlugt, "Diffusion coefficients from molecular dynamics simulations in binary and ternary mixtures," Int. J. Thermophys. **34**, 1169 (2013).
[23]A. Ben-Naim, "Theoretical aspects of self-assembly of proteins: A Kirkwood-Buff-theory approach," J. Chem. Phys. **138**(22), 224906 (2013).
[24]M. B. Gee and P. E. Smith, "Kirkwood–Buff theory of molecular and protein association, aggregation, and cellular crowding," J. Chem. Phys. **131**(16), 165101 (2009).
[25]E. E. Bruce, H. I. Okur, S. Stegmaier, C. I. Drexler, B. A. Rogers, N. F. A. van der Vegt, S. Roke, and P. S. Cremer, "Molecular mechanism for the interactions of Hofmeister cations with macromolecules in aqueous solution," J. Am. Chem. Soc. **142**(45), 19094–19100 (2020).
[26]P. Kumari, V. V. S. Pillai, D. Gobbo, P. Ballone, and A. Benedetto, "The transition from salt-in-water to water-in-salt nanostructures in water solutions of organic ionic liquids relevant for biological applications," Phys. Chem. Chem. Phys. **23**, 944–959 (2021).
[27]M. B. Gee, N. R. Cox, Y. Jiao, N. Bentenitis, S. Weerasinghe, and P. E. Smith, "A Kirkwood-Buff derived force field for aqueous alkali halides," J. Chem. Theory Comput. **7**(5), 1369–1380 (2011).
[28]M. Fyta, "Structural and technical details of the Kirkwood-Buff integrals from the optimization of ionic force fields: Focus on fluorides," Eur. Phys. J. E **35**(3), 21 (2012).
[29]E. Schneck, D. Horinek, and R. R. Netz, "Insight into the molecular mechanisms of protein stabilizing osmolytes from global force-field variations," J. Phys. Chem. B **117**(28), 8310–8321 (2013).
[30]P. Loche, P. Steinbrunner, S. Friedowitz, R. R. Netz, and D. J. Bonthuis, "Transferable ion force fields in water from a simultaneous optimization of ion solvation and ion–ion interaction," J. Phys. Chem. B **125**(30), 8581–8587 (2021).
[31]P. Ganguly, D. Mukherji, C. Junghans, and N. F. A. van der Vegt, "Kirkwood–Buff coarse-grained force fields for aqueous solutions," J. Chem. Theory Comput. **8**(5), 1802–1807 (2012).
[32]T. E. de Oliveira, P. A. Netz, K. Kremer, C. Junghans, and D. Mukherji, "C–IBI: Targeting cumulative coordination within an iterative protocol to derive coarse-grained models of (multi-component) complex fluids," J. Chem. Phys. **144**(17), 174106 (2016).
[33]P. Krüger, "Validity of the compressibility equation and Kirkwood-Buff theory for crystalline matter," Phys. Rev. E **103**, L061301 (2021).
[34]M. Miyaji, B. Radola, J.-M. Simon, and P. Krüger, "Extension of Kirkwood–Buff theory to solids and its application to the compressibility of fcc argon," J. Chem. Phys. **154**(16), 164506 (2021).
[35]T. L. Hill, *Thermodynamics of Small Systems* (Dover, 1963).
[36]L. D. Site, G. Ciccotti, and C. Hartmann, "Partitioning a macroscopic system into independent subsystems," J. Stat. Mech.: Theory Exp. **2017**(8), 083201.
[37]M. Rovere, D. W. Hermann, and K. Binder, "Block density distribution function analysis of two-dimensional Lennard-Jones fluids," Europhys. Lett. **6**(7), 585 (1988).
[38]M. Rovere, D. W. Heermann, and K. Binder, "The gas-liquid transition of the two-dimensional Lennard-Jones fluid," J. Phys.: Condens. Matter **2**(33), 7009 (1990).
[39]F. L. Román, J. A. White, and S. Velasco, "Fluctuations in an equilibrium hard-disk fluid: Explicit size effects," J. Chem. Phys. **107**, 4635 (1997).
[40]S. K. Schnell, T. J. H. Vlugt, J.-M. Simon, B. Dick, and S. Kjelstrup, "Thermodynamics of a small system in a μt reservoir," Chem. Phys. Lett. **504**(4–6), 199–201 (2011).
[41]S. K. Schnell, X. Liu, J.-M. Simon, A. Bardow, D. Bedeaux, T. J. H. Vlugt, and S. Kjelstrup, "Calculating thermodynamic properties from fluctuations at small scales," J. Phys. Chem. B **115**(37), 10911–10918 (2011).
[42]P. Krüger, S. K. Schnell, D. Bedeaux, S. Kjelstrup, T. J. H. Vlugt, and J.-M. Simon, "Kirkwood-Buff integrals for finite volumes," J. Phys. Chem. Lett. **4**(2), 235–238 (2013).
[43]P. Ganguly and N. F. A. van der Vegt, "Convergence of sampling Kirkwood-Buff integrals of aqueous solutions with molecular dynamics simulations," J. Chem. Theory Comput. **9**(3), 1347–1355 (2013).
[44]P. Krüger and T. J. H. Vlugt, "Size and shape dependence of finite-volume Kirkwood-Buff integrals," Phys. Rev. E **97**, 051301 (2018).
[45]A. Santos, "Finite-size estimates of Kirkwood-Buff and similar integrals," Phys. Rev. E **98**, 063302 (2018).
[46]R. Cortes-Huerto, K. Kremer, and R. Potestio, "Communication: Kirkwood-Buff integrals in the thermodynamic limit from small-sized molecular dynamics simulations," J. Chem. Phys. **145**(14), 141103 (2016).
[47]F. L. Román, J. A. White, A. González, and S. Velasco, "Fluctuations in a small hard-disk system: Implicit finite size effects," J. Chem. Phys. **110**(20), 9821–9824 (1999).
[48]F. L. Román, J. A. White, A. González, and S. Velasco, "Ensemble effects in small systems," in *Theory and Simulation of Hard-Sphere Fluids and Related Systems* (Springer, Berlin, Heidelberg, 2008), pp. 343–381.
[49]D. Villamaina and E. Trizac, "Thinking outside the box: Fluctuations and finite size effects," Eur. J. Phys. **35**(3), 035011 (2014).
[50]N. W. Ashcroft and D. C. Langreth, "Structure of binary liquid mixtures. I," Phys. Rev. **156**, 685–692 (1967).
[51]W. Härtl, C. Segschneider, H. Versmold, and P. Linse, "On the structure factor of liquid-like ordered binary mixtures of colloidal suspensions," Mol. Phys. **73**(3), 541–552 (1991).
[52]J.-P. Hansen and I. R. McDonald, *Theory of Simple Liquids* (Elsevier, 1990).
[53]F. Sedlmeier, D. Horinek, and R. R. Netz, "Spatial correlations of density and structural fluctuations in liquid water: A comparative simulation study," J. Am. Chem. Soc. **133**(5), 1391–1398 (2011).
[54]H. J. C. Berendsen, J. R. Grigera, and T. P. Straatsma, "The missing term in effective pair potentials," J. Phys. Chem. **91**(24), 6269–6271 (1987); L. X. Dang and B. M. Pettitt, "Simple intramolecular model potentials for water," *ibid.* **91**(12), 3349–3354 (1987); Y. Wu, H. L. Tepper, and G. A. Voth, "Flexible simple point-charge water model with improved liquid-state properties," J. Chem. Phys. **124**(2), 024503 (2006).
[55]S. Pronk, S. Páll, R. Schulz, P. Larsson, P. Bjelkmar, R. Apostolov, M. R. Shirts, J. C. Smith, P. M. Kasson, D. van der Spoel, B. Hess, and E. Lindahl, "GROMACS 4.5: A high-throughput and highly parallel open source molecular simulation toolkit," Bioinformatics **29**(7), 845–854 (2013).
[56]H. J. C. Berendsen, J. P. M. Postma, W. F. van Gunsteren, A. DiNola, and J. R. Haak, J. Chem. Phys. **81**, 3684 (1984).
[57]G. Bussi, D. Donadio, and M. Parrinello, "Canonical sampling through velocity rescaling," J. Chem. Phys. **126**(1), 014101 (2007).
[58]S. Weerasinghe and P. E. Smith, "A Kirkwood-Buff derived force field for mixtures of urea and water," J. Phys. Chem. B **107**(16), 3891–3898 (2003).
[59]K. Binder, "Finite size scaling analysis of Ising model block distribution functions," Z. Phys. B **43**(2), 119–140 (1981).
[60]J. J. Salacuse, A. R. Denton, and P. A. Egelstaff, "Finite-size effects in molecular dynamics simulations: Static structure factor and compressibility. I. Theoretical method," Phys. Rev. E **53**, 2382–2389 (1996).
[61]F. L. Román, J. A. White, and S. Velasco, "Block analysis method in off-lattice fluids," Europhys. Lett. **42**(4), 371 (1998).
[62]J. L. Lebowitz and J. K. Percus, "Long-range correlations in a closed system with applications to nonuniform fluids," Phys. Rev. **122**, 1675–1691 (1961).
[63]H. Kokubo, J. Rösgen, D. W. Bolen, and B. M. Pettitt, "Molecular basis of the apparent near ideality of urea solutions," Biophys. J. **93**(10), 3392–3407 (2007).
[64]L. A. Baptista, R. C. Dutta, M. Sevilla, M. Heidari, R. Potestio, K. Kremer, and R. Cortes-Huerto, "Density-functional-theory approach to the Hamiltonian adaptive resolution simulation method," J. Phys.: Condens. Matter **33**, 184003 (2021).